Multifaceted asymmetric radiation from the edge-like asymmetric radiative collapse of density limited plasmas in the Large Helical Device

B. J. Peterson, Yuhong Xu, S. Sudo, T. Tokuzawa, K. Tanaka et al.

Related Articles

Toroidal precession as a geometric phase
Phys. Plasmas 20, 012511 (2013)

Toroidal magnetized plasma device with sheared magnetic field lines using an internal ring conductor
Rev. Sci. Instrum. 84, 013504 (2013)

Linear properties of energetic particle driven geodesic acoustic mode
Phys. Plasmas 20, 012506 (2013)

Gyrokinetic studies of the effect of β on drift-wave stability in the National Compact Stellarator Experiment
Phys. Plasmas 19, 122306 (2012)

Spontaneous healing and growth of locked magnetic island chains in toroidal plasmas
Phys. Plasmas 19, 112501 (2012)
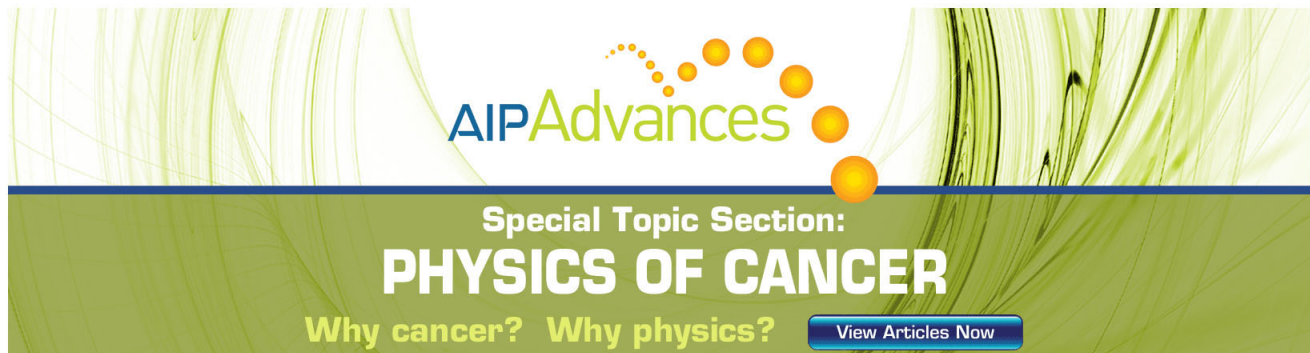
Additional information on Phys. Plasmas

Journal Homepage: http://pop.aip.org/

Journal Information: http://pop.aip.org/about/about_the_journal

Top downloads: http://pop.aip.org/features/most_downloaded

Information for Authors: http://pop.aip.org/authors

Multifaceted asymmetric radiation from the edge-like asymmetric radiative collapse of density limited plasmas in the Large Helical Device

B. J. Peterson,[a] Yuhong Xu, S. Sudo, T. Tokuzawa, K. Tanaka, M. Osakabe, S. Morita,
M. Goto, S. Sakakibara, J. Miyazawa, K. Kawahata, N. Ohyabu, H. Yamada,
O. Kaneko, A. Komori, and the LHD Experimental Group

National Institute for Fusion Science, Toki-shi, Gifu-ken 509-5292, Japan

Neutral beam injection heated discharges at the density limit in the Large Helical Device [O. Motojima, H. Yamada, A. Komori *et al.*, Phys. Plasmas **6**, 1843 (1999)] are terminated with asymmetric radiative collapse (ARC) exhibiting several properties in common with the MARFE (multifaceted asymmetric radiation from the edge) phenomenon: (1) A highly poloidally asymmetric radiation profile which is stronger on the inboard side. (2) This asymmetry is well correlated with the signal from the multichord interferometer. (3) Moreover, evidence from several diagnostics at different toroidal locations supports the possibility that ARC may be toroidally symmetric. However in contrast to MARFE, ARC is only observed in the period just prior to the quench of the plasma. © *2001 American Institute of Physics.* [DOI: 10.1063/1.1390330]

Density limit is one of the most important issues in both tokamaks and heliotron/stellarator devices whose goal is the achievement of thermonuclear fusion conditions.[1–3] In helical devices, the radiation-induced density limit has particular importance, since it is a main cause leading to collapse of the plasma when the radiated power increased with density exceeds the deposited power.[3,4] This type of density limit is thought to be related to the onset of an edge thermal instability arising from the increase of impurity radiation with reduced temperature.[5–7] In tokamaks, radiative collapse may result in a cooling of the plasma boundary resulting in a contraction of the plasma. Additionally, a poloidally symmetric radiating belt is generally established in such radiative collapse discharges.[1,8,9] Meanwhile, MARFE (multifaceted asymmetric radiation from the edge), which is an axisymmetric zone of high radiation located at the inner side of the torus, has been observed frequently in tokamaks.[1,8,10,11] Physics of the density limit in the context of MARFE formation has been intensively studied theoretically.[12–15] It is suggested that MARFEs might be caused by a poloidally asymmetric radial heat and particle flow due to Shafranov shift or by the poloidally asymmetric recycling properties resulting from proximity of the first wall on the inboard side.[1,16] In toroidal helical plasmas, much attention has been paid recently to the radiation-induced density limit phenomenon.[2–4,17–22] However, the experimental results of the radiation structure have rarely been reported in helical devices. In this Letter, we make the first report of asymmetric radiative collapse in the Large Helical Device (LHD) and relate asymmetric radiative collapse to the MARFE phenomenon commonly observed in tokamaks and to the density limit in LHD.

LHD is a superconducting heliotron system with a $l/m = 2/10$ helical coil set. For the discharges in this study LHD was heated with 1–3 MW of neutral beam injection (NBI) with $R/a = 3.6$–$3.75/0.6$ m, $B_t = 1.5$–2.75 T, $n_e = 0.6$–7.0×10^{19}/m^3, $T_e = 0.5$–2 keV, and $T_i = 0.5$–2 keV.[23] Bolometer arrays used for the diagnosis of the total plasma radiation profiles include one 20-channel resistive metal film bolometer array installed at a bottom port with 14 channels viewing the vertically elongated poloidal cross section of the core.[22] At a horizontal midplane port, another 16-channel bolometer array was mounted viewing the horizontally elongated cross section of the plasma. The temporal resolution of the bolometers is 5 ms.

In LHD, the discharges are usually terminated in two ways: (1) thermal decay after the termination of NBI and (2) radiative collapse during the NBI. It was found that for the thermal decay and radiative collapse discharges the plasma radiation profile was usually poloidally symmetric and asymmetric, respectively. These occurred independent of the wall conditioning such as glow discharge or Ti-gettering. In this Letter we focus on the description of radiative collapse in LHD, similarities to MARFE, and its relation to the density limit.

In Fig. 1, typical wave forms of the so-called radiative collapse are displayed. From Fig. 1(b) it can be seen that the line-averaged electron density, n_e, keeps increasing with the gas puffing for the duration of the discharge and only decreases after the stored energy becomes very small. This type of low temperature, moderate density plasma is commonly observed in LHD and is possible due to the zero net-current, disruption-free characteristics of helical devices. Because the total radiated power, P_{rad}, is essentially a result of impurity radiation, P_{rad} is determined by n_e, impurity density, n_z, and the impurity cooling rate, $L_z(T_e)$, i.e., $P_{rad} = \Sigma_Z n_e n_z L_z(T_e)$. Therefore an increase of n_e will enhance P_{rad} for each of the impurities. The gradual linear increase of P_{rad} from O$_V$ and C$_{III}$ can be seen in Figs. 1(c) and 1(d) before 0.86 s, at which time W_p begins to decrease rapidly.
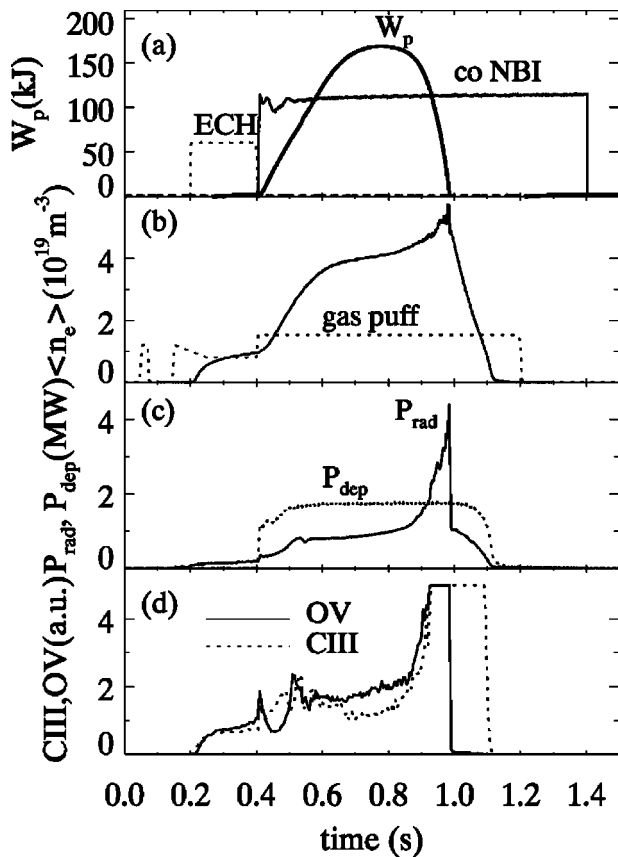
FIG. 1. Typical wave forms of a radiative collapse discharge (shot 3574) (a) total plasma stored energy and ECH and NBI timing, (b) line-averaged density and gas-puff timing, (c) total radiated power and deposited NBI power and (d) spectroscopy signals from OV and CIII.
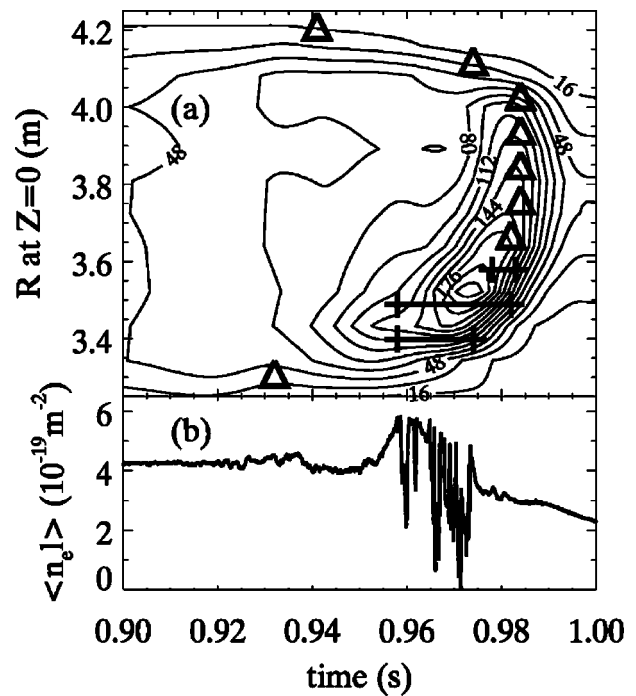

FIG. 2. (a) Comparison of bolometer brightness (W/m^2) profile evolution (contours) and FIR interferometer data for the shot shown in Fig. 1. The peaks in FIR line densities are shown with triangles. The periods of signal degradation for three of the inboard FIR channels are also shown (two plus signs). (b) Line density evolution for the FIR interferometer chord at $R = 3.4$ m.

The rapid drop of W_p occurs after the continuously increasing P_{rad} exceeds the net absorbed power (NBI deposited power minus other power losses which are not shown in Fig. 1). At the same time, the increase of P_{rad} cools the plasma boundary. For the intrinsic low-Z impurities of O and C in the edge area, a reduction of the local temperature leads to an increase of $L_z(T_e)$ and thus P_{rad}, which may further reduce the temperature. This is the so-called thermal or radiative instability.[5–7] In the discharge presented, the trigger of this thermal instability is marked by the sharp jumps in O_V and C_{III} signals at about $t = 0.86$ s. The enhanced impurity radiation results in a substantial increase of P_{rad}, as seen in Fig. 1(c). The instability proceeds with an acceleration in the drop of W_p (and consequently T_e) and the rapid increase of P_{rad} until the plasma prematurely collapses at $t = 1.00$ s, well before the switch-off of NBI. This collapse is followed by a cold plasma from which the primary radiation is from carbon and which dissipates after approximately 100 ms.

The sharp increase in the radiation prior to the end of the discharge motivates us to further investigate the radiation distribution features during this period. Figure 2(a) displays the late-period time evolution of the chord-integrated radiation brightness for the same radiative collapse discharge as shown in Fig. 1. From Fig. 2(a), we can see that prior to the loss of power balance at $t = 0.92$ s [as indicated by $P_{rad} > P_{dep}$ in Fig. 1(c)], the radiation profile is rather symmetric.

However, after this time the radiation gradually becomes asymmetric beginning at about 0.94 s at which time the increase of radiation on the inboard side is much more drastic than that on the outboard side. Global measurements of $H\alpha$ showing it increasing after the appearance of the radiation asymmetry indicate that recycling from the wall (4 cm away from plasma at nearest location on inboard side for $R_{axis} = 3.75$ m) may be contributing to the asymmetry, but is not triggering it. This shows that the radiation during radiative collapse discharges in LHD is poloidally asymmetric prior to the final collapse, similar to the MARFEs observed in tokamaks.

Another signature of MARFE is observed in the comparison between the density signals measured by multichord far infrared (FIR) interferometer ($\lambda = 119\ \mu$m)[24] and the bolometer array signals both from vertically elongated cross sections that are separated by a toroidal angle $\phi \sim 72°$ (two field periods). In Fig. 2(a) the time of the peak of the line density signals obtained from each of vertical FIR channels is also shown by a triangle. In the case of three of the inboard channels the interferometer signal is degraded due to the reduction of the beat signal amplitude of the heterodyne interferometer. An example of this degradation is shown in the line density signal of the FIR chord at $R = 3.4$ m in Fig. 2(b), while an example of a normal, undegraded signal is shown by the line-averaged density signal from the central FIR chord at $R = 3.76$ m in Fig. 1(b). The cause of this signal amplitude reduction is most likely the deflection of the laser beam due to high density gradients. The period when each of these three channels experiences this signal degradation is
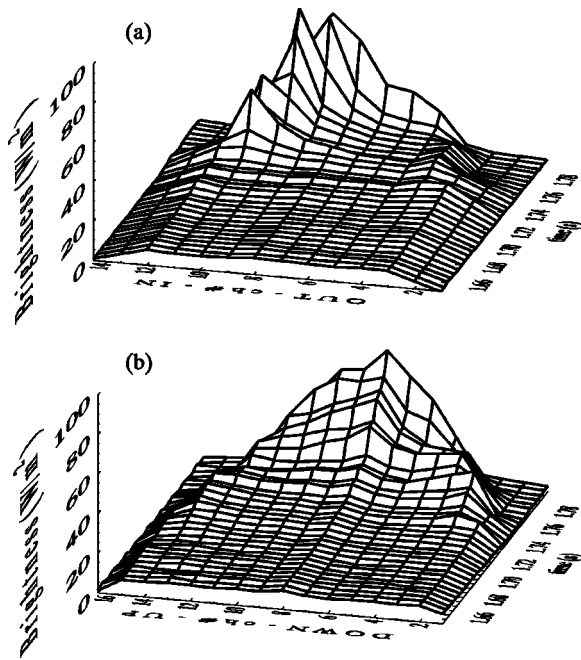
FIG. 3. Time evolution of the radiation brightness profile for a radiative collapse shot (shot 10272) measured at (a) the vertically elongated cross section and (b) the horizontally elongated cross section.
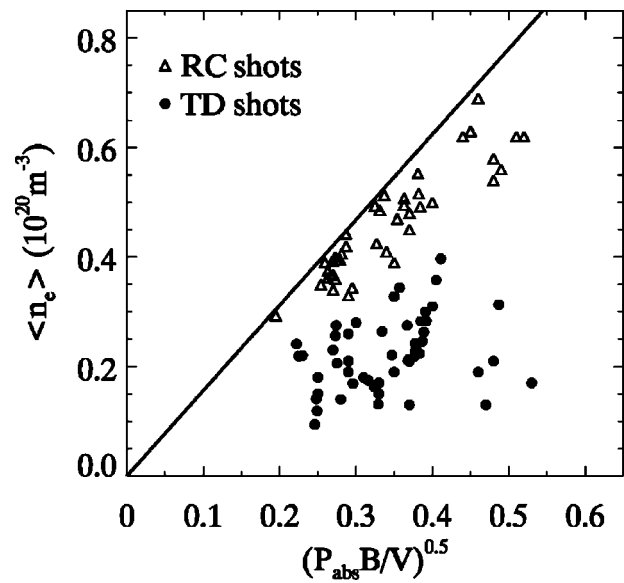

FIG. 4. Line-averaged density scaling for discharges terminated by radiative collapse (open triangles) and thermal decay (closed circles) and upper limit of radiative collapse line-averaged density (solid line).

shown in Fig. 2(a) by two plus signs connected by a line. Good spatial and temporal correlation can be observed between the highly asymmetric radiation and the peaks in the density signals. Also the period of signal degradation on three of the inboard channels coincides with the asymmetric peak in the bolometer signal. This is similar to the phenomenon that has been observed during MARFE in tokamaks.[8,10]

In tokamaks, the poloidally asymmetric MARFE has often been observed as a toroidally symmetric phenomena. Since the magnetic field configuration and wall structure in a helical device differ much from that in a tokamak, it is of great interest to investigate the radiation structure at different toroidal angles in LHD. The two elliptic shaped cross sections at the vertical port (vertically elongated, viewed from the bottom) and the horizontal port (horizontally elongated, viewed from the outboard side) are each viewed by a bolometer array and are separated by a toroidal angle $\phi \sim 50°$ (1.4 field periods). The sight lines of the two arrays allow them to simultaneously view the radiation from the inboard and outboard sides on the vertical port and from the upper and lower sides on the horizontal port. The measurements of the time evolution of the radiation profile for a radiative collapse shot on these two ports are shown in Fig. 3. From Fig. 3(a), during the collapse a clearly poloidally asymmetric radiation distribution, which is similar to that shown in Fig. 2, can be observed at the vertical cross section between the in- and outboard sides. However, in Fig. 3(b) the radiation at the horizontal cross section exhibits a structure which is quite symmetric between the upper (detected by channels 9–15) and lower (detected by channels 2–8) sides. In addition, the poloidal asymmetry is observed at another toroidal location in the line density measurements made by the FIR interferometer discussed previously. These results indicate that the

poloidally asymmetric radiation in LHD may also be toroidally symmetric similar to a MARFE in a tokamak. However, we cannot definitely conclude that the poloidal asymmetry in the radiation is axisymmetric as the array at the horizontal port does not give us any information on the major radial profile of the radiation (whether it peaks in the center, on the inboard or outboard sides).

As discussed previously, radiative collapse should be closely linked to the density limit in LHD. When the density in the plasma exceeds a certain value, depending on the heating power and other parameters, an excessive radiated power loss will lead to a premature termination of the discharge due to radiative collapse of the plasma.[1–3,9] An empirical scaling law has been proposed for the maximum achievable mean density in Heliotron-E: $\bar{n}_c(10^{20}\,\mathrm{m}^{-3}) = 0.25(P_{abs}B/a^2R)^{0.5} \cong 1.11(P_{abs}B/V)^{0.5}$, where $P_{abs}(\mathrm{MW})$, $B(T)$, and $V(\mathrm{m}^3)$ are the absorbed power, magnetic field, and plasma volume, respectively.[2] More recently, a similar form of the scaling law was given for W7-AS with $\bar{n}_c(10^{20}\,\mathrm{m}^{-3}) \cong 1.46(P_{abs}/V)^{0.48}B^{0.54}$.[3] These scaling laws are in basic agreement with theoretical models.[17,21] In order to compare our experimental data with the scaling laws for other helical machines, a plot of $\bar{n}_e$ as a function of the volume-averaged absorbed power and magnetic field, $(P_{abs}B/V)^{0.5}$, is shown in Fig. 4 for both the thermal decay and radiative collapse discharges. The data are taken at the time of maximum plasma stored energy. A line showing the limit of the radiative collapse shots is also plotted in Fig. 4 with the formula of $\bar{n}_c(10^{20}\,\mathrm{m}^{-3}) = 1.56(P_{abs}B/V)^{0.5}$. Figure 4 also shows that the density level of the thermal decay shots (closed points) is well below those of the collapsing shots, indicating that discharges having a symmetric radiative termination occur at densities well below the density limit. This result explicitly indicates that asymmetric radiative collapse of the plasma on LHD occurs in discharges with a density approaching a density limit which is consistent with the density scaling laws

achieved in other helical systems. However it should be noted that the asymmetery in the radiation develops well after the time when the density limit is reached as indicated by the peak in the stored energy. This suggests that the asymmetry is not the cause of the collapse but rather follows from it.

We have reported on radiative collapse in LHD, which occurs prior to the NBI termination as a result of the plasma reaching the density limit when the radiated power exceeds the NBI deposited power. In the case of thermal decay, when the discharge is terminated with the NBI, the radiation profile is typically inboard–outboard symmetric and the density is below the density limit, while discharges prematurely terminated by radiative collapse at the density limit have radiation profiles which become poloidally asymmetric on the inboard side in the final stages of the collapse. In addition to this poloidally asymmetric radiation pattern the radiative collapse phenomenon is similar to MARFE in tokamaks in that a degradation of the interferometer signal on three of the inboard channels is observed which coincides spatially and temporally with the asymmetric peak in the bolometer signal. Data from this interferometer array and another bolometer array mounted at a horizontal midplane port indicate that this asymmetry might be axisymmetric like a MARFE in a tokamak; however the definite determination of this is left to future measurements of the two- and three-dimensional radiation distribution using tomographic analysis of data from multiple bolometer arrays. Furthermore, the density achieved by these asymmetric radiative collapse discharges at the peak in the stored energy obeys a scaling law which is similar to that seen in other helical devices. This work is not intended as a definitive study of density limit scaling in LHD, as only a linear fit was made, neglecting the power fitting of the absorbed power, magnetic field, and plasma volume. Also, the data set included only gas puff and neutral beam fueled discharges (no pellet fueled discharges). A more detailed study including the wide variation of these parameters and pellet-fueled discharges is left to the future.

While asymmetric radiative collapse has many properties in common with MARFE, to this point it has only been observed in LHD as a transient phenomenon just prior to the termination of discharges at the density limit, while MARFE in tokamaks has been observed to persist for several hundreds of milliseconds and does not necessarily lead to the termination of the discharge. We plan to study the mechanism of this phenomenon in more depth in the future, considering what the source of this asymmetry might be especially in terms of its three-dimensional structure and its relation to the thermal instability that precedes it.

[1] J. Rapp, P. C. De Vries, F. C. Schueller *et al.*, Nucl. Fusion **39**, 765 (1999).
[2] S. Sudo, Y. Takeiri, H. Zushi, F. Sano, K. Itoh, K. Kondo, and A. Iiyoshi, Nucl. Fusion **30**, 11 (1990).
[3] L. Giannone, J. Baldzuhn, R. Burhenn *et al.*, Plasma Phys. Controlled Fusion **42**, 603 (2000).
[4] H. Wobig, Plasma Phys. Controlled Fusion **42**, 931 (2000).
[5] N. Ohyabu, Nucl. Fusion **9**, 1491 (1979).
[6] D. E. T. F. Ashby and M. H. Hughes, Nucl. Fusion **21**, 911 (1981).
[7] W. M. Stacey, Phys. Plasmas **4**, 1069 (1997).
[8] B. Lipschultz, J. Nucl. Mater. **145−147**, 15 (1987).
[9] J. A. Wesson, R. D. Gill, M. Hugon *et al.*, Nucl. Fusion **29**, 641 (1989).
[10] B. Lipschultz, B. LaBombard, E. S. Marmar, M. M. Pickrell, J. L. Terry, R. Watterson, and S. M. Wolfe, Nucl. Fusion **24**, 977 (1984).
[11] T. Nishitani, S. Ishida, N. Hosogane, T. Sugie, K. Itami, and H. Takeuchi, J. Nucl. Mater. **176−177**, 763 (1990).
[12] T. E. Stringer, *Proceedings of the 12th European Conference on Controlled Fusion and Plasma Physics, Budapest, 1985* (European Physical Society, Petit-Lancy, 1985), Vol. 9F-I, p. 86.
[13] W. M. Stacey, Plasma Phys. Controlled Fusion **39**, 1245 (1997).
[14] J. Neuhauser, W. Schneider, and R. Wunderlich, Nucl. Fusion **26**, 1679 (1986).
[15] W. M. Stacey and T. W. Petrie, Phys. Plasmas **7**, 4931 (2000).
[16] G. Sergienko, K. Hoethker, A. Nedospasov *et al.*, *Proceedings of the 20th European Conference on Controlled Fusion and Plasma Physics, Lisbon, 1993* (European Physical Society, Geneva, 1993), Vol. 17C, Part II, p. 667.
[17] K. Itoh and S.-I. Itoh, J. Phys. Soc. Jpn. **57**, 1269 (1988).
[18] F. Wagner, J. Baldzuhn, R. Brakel *et al.*, Plasma Phys. Controlled Fusion **36**, A61 (1994).
[19] L. Giannone, R. Burhenn, P. Grigull *et al.*, J. Nucl. Mater. **266−269**, 507 (1999).
[20] Y. Takeiri, Y. Nakamura, N. Noda *et al.*, Plasma Phys. Controlled Fusion **42**, 147 (2000).
[21] K. Itoh, S.-I. Itoh, and L. Giannone, Research Report No. NIFS-627.
[22] B. J. Peterson, K. Y. Watanabe, M. Osakabe *et al.*, *Proceedings of the 26th European Conference on Controlled Fusion and Plasma Physics, Maastricht, 1999* (European Physical Society, Geneva, 1999), Vol. 23J, p. 1337.
[23] O. Motojima, H. Yamada, A. Komori *et al.*, Phys. Plasmas **6**, 1843 (1999).
[24] K. Kawahata, K. Tanaka, Y. Ito, A. Ejiri, and S. Okajima, Rev. Sci. Instrum. **70**, 707 (1999).